Community detection within edge exchangeable models for interaction processes

Yuhua Zhang, Walter Dempsey

October. 1, 2021

Abstract

Health scientists are increasingly interested in discovering community structure from peer-to-peer support networks. While many methods have been proposed for finding community structure, few account for the fact that these modern networks arise from processes of interactions in the population such as user post and comment exchanges. We introduce cluster-wise edge exchangeable models for the study of interaction networks with latent community structure. We use the cluster-wise vertex components model (C-VCM) as a canonical example. Several theoretical and practical advantages over traditional vertex-centric approaches are highlighted. In particular, cluster-wise edge exchangeable models allow for sparse degree structure and power-law degree distributions within communities. Our theoretical analysis bounds the misspecification rate of cluster assignments, while supporting simulations show the properties of the network can be recovered. A computationally tractable Gibbs algorithm is derived. We demonstrate the proposed model using post-comment interaction data from Talklife, a large-scale online peer-to-peer support network.

Keywords— Large-scale Sparse Network, Edge Exchangeable Model, Community Detection, Interaction Process, Power-law Degree Distribution

1 Introduction

The WorldWideWeb, social media, and technological innovation allow people from around the world to easily interact across geographical, cultural and economic boundaries. Among its many benefits, increased connectivity enhances information flow, promotes community building, and facilitates the formation of support systems for individuals struggling with illness and addiction. In this paper, we focus on network data arising from sequences of interactions collected on social media platforms such as peer-to-peer support networks. In suicide research, for example, social support has been shown to be a preventative factor for future suicidal ideation [12]. To further these goals, this paper focuses on discovery of latent community structure.

An increasingly popular class of models for community detection are the stochastic block models (SBMs) [10]. The basic version of the SBM assumes vertices within the same block have the same probability of forming an edge (i.e., interact) with other vertices, and within-cluster interactions are more likely than between-cluster interactions. Many associated methods have been proposed. These include but are not limited to spectral clustering based methods ([18], [3]), Bayesian methods ([15], [13]), and pseudo-likelihood based methods ([2], [20]). The stochastic block model was later generalized to the degree-corrected stochastic block model (DCSBM) [11], which allows for vertex degree heterogeneity. Theoretical guarantees of community recovery have been well established [7, 2, 28].

As mentioned in the previous literature[1], the power law degree distributions are observed in many communication and social networks. That is, many real-world networks contain a few high degree nodes and many low degree nodes. This network feature can be leveraged when detecting underlying community structure. Efforts have been made, for example, to adapt the SBM to allow for power-law degree distributions [17]. Though much progress has been made, SBM and its extensions do not account for the fact that modern networks arise from processes of interactions. On the other hand, edge-exchangeable models [5, 4] were built specifically to analyze such interaction datasets, incorporating power-law structure and network sparsity into model formulation. While edge-exchangeable models offer an attractive theoretical framework, the current set of edge exchangeable models do not account for latent community structure.

The model proposed in this paper is motivated by this important fact: most common complex networks constructed from interaction data exhibit community structure. Prior edge exchangeable models focus mainly on the inference of network statistics, without considerations of community structure. Here, we propose a new model which extends edge exchangeability framework to allow community structure while permitting power-law degree and sparsity.

1.1 Outline and main contributions

The main contribution of this paper is organized in the following way. We start by formally defining the network data and notations in Definition 2.2. The generative process of the interaction data is then described in Section 2.3. A computationally tractable Gibbs sampling inferential algorithm is derived in Section 3.1. Simulation results that support our models ability to capture power-law degree distributions and community structure are presented in Section 3.2. We then consider application of our method to a peer-to-peer mental health support network in Section 4. We end with a summary of the proposed methods and implications in Section 5.

2 Cluster-wise Edge Exchangeable Model

2.1 Motivating Example

Our motivating example is TalkLife, a large-scale online peer support network for mental health. Talklife's users post short text snippets to which other users can react and/or comment. Each post consists of a poster and a set of commentators. Every post is flagged using machine-learning classifiers with at least one health-related topic, e..g, Anxiety/ Panic/ Fear suspected, Body Image/ Eating Disorders suspected and so on. The platform has collected millions of interactions among its users. A primary purpose of TalkLife is to strengthen its peer support networks and improve mental health outcome for its users. The network is of complex structures, and viewing the entire dataset as a whole network will lead to the loss of many features of the interactions among the users. Therefore, a natural question that arise is how to break the entire dataset into smaller groups and identify certain groups of people from the interaction data.

2.2 Notation and Data

We start by defining cluster-structured interaction data. Inspired by the previous work [4], we extend the definition of interaction data to the setting where there exists an underlying cluster structure. To start, we use a simple example based on Talklife. Recall each Talklife post consists of a poster s and a set of commentators $\{r_1, \ldots, r_k\}$. Then a post on Talklife can be summarized by the ordered pair $\{\{s\}, \{r_1, \ldots, r_k\}\}$. See Figure 1 for a visualization taking in the Talklife data and constructing the ordered pairs for a set of posts. Here, posters and commentators are drawn from the same underlying population, which we denote $\mathcal{P} \subset \mathbb{N}$. Definition 2.1 formalizes this example into a general definition of interaction data.

Definition 2.1 (Interaction data) For a set $\mathcal{P}$, let $fin(\mathcal{P})$ be the multisets of all finite subsets of $\mathcal{P}$. The interaction process of $\mathcal{P}$ is the correspondence $\mathcal{I} : \mathbb{N} \to fin(\mathcal{P})$ between the natural numbers and finite subsets of $\mathcal{P}$.

Additional structure can be incorporated into Definition 2.1. In Talklife, for example, there is a single poster and multiple commentators. Definition 2.1 can capture this by replacing $fin(\mathcal{P})$ with $fin_1(\mathcal{P}) \times fin(\mathcal{P})$ where $fin_1(\mathcal{P})$ are sets of size one from $\mathcal{P}$. See [5] for additional examples of these extensions. Note that the nodes are labeled in the order of appearance. If a new individual is chosen, that person is given the next label in the order of appearance. For example, if they are the 10th person to be observed, they are labelled as individual 10.

Using Figure 1 as an example, each interaction is represented by the user who posts and the users who comment. The users, regardless of being posters or commentators, are drawn from the population $\mathcal{P}$ set equal to $\mathbb{N}$. The interaction process is a correspondence $\mathcal{I} : \mathbb{N} \to fin_1(\mathbb{N}) \times fin(\mathbb{N})$. For Post 1, $\mathcal{I}(1) = (\{1\},\{3, 4, 5\})$ representing the poster posted by User 1 being commented by User 3, 4, and 5. The second Post $\mathcal{I}(2) = (\{2\},\{6, 7\})$ represents User 2 posts and User 6 and 7 comment.

Under our model assumption, individuals who are from the same cluster have more frequent interactions with the users from the same cluster as compared to other users. In Figure 1, for example, User 3, 4, and 5 are in the same cluster, which leads to a higher likelihood of observing these individuals commentating on a post by User 1. User 8 and User 9 are in a separate cluster,

which explains the second interaction. Note, however, that users in distinct clusters may comment on each other's posts, i.e., User 7 comments on a post by User 2. We formalize community structure in interaction data in Definition 2.2.

Definition 2.2 (Cluster structured interaction data) A *K-cluster structure* is defined as the mapping $B : \mathcal{P} \to [K]$, such that for all $x \in \mathcal{P}$, $B(x) \in [K]$ is the cluster that x is assigned. The interaction process induced by B is called the *cluster interaction process*, which is the correspondence $\mathcal{I}_B : \mathbb{N} \to fin([K])$.

In our running example shown in Figure 1, $K = 2$ and the interaction process induced by B is $\mathcal{I}_B(1) = (\{1\}, \{1, 1, 1\})$ for Post 1, and $\mathcal{I}_B(2) = (\{1\}, \{1, 2\})$ for Post 2, and $\mathcal{I}_B(3) = (\{2\}, \{2, 2\})$ for Post 3. Note that for the pre-image B^{-1}, $B^{-1}(i) \cap B^{-1}(j) = \emptyset$ if $i \neq j$, and $B^{-1}(i) = B^{-1}(j)$ if $i = j$ for $i, j \in [K]$. That is, B partitions $\mathcal{P}$ into K non-overlapping sets.

In the remainder of the paper, we write $\mathcal{Y}_m$ to indicate the observed network with edges labeled in $m \in \mathbb{N}$, and $E_1, E_2, \ldots, E_m$ as the interactions observed, where $E_j = (\{S_j, C_j^{(s)}\}, \{R_j, C_j^{(r)}\})$, $j \in [m]$, that is, the interaction j is initiated from the sender S_j of cluster $C_j^{(s)}$ and points to the receiver R_j of cluster $C_j^{(r)}$. Let $v(\mathcal{Y}_m)$ be the number of vertices in the network, and $m(\mathcal{Y}_m)$ be the total degree of the network. Note that $m(\mathcal{Y}_m) = 2m$. We subscript $c \in [K]$ to indicate the cluster specific variables. For example, $m(\mathcal{Y}_c)$ is the total degree of cluster c. We now give the definition of the cluster edge exchangeable network.

Definition 2.3 (Cluster edge exchangeable network) The network constructed from interactions within the same cluster $\mathcal{Y}_c \subset \mathcal{Y}_m$, $c \in [K]$, is exchangeable if $\mathcal{Y}_c^{\sigma} =_D \mathcal{Y}_c$, for all permutations $\sigma : \mathcal{P} \to \mathcal{P}$ where $=_D$ denotes equality in distribution. We say an interaction process is cluster edge exchangeable if this definition holds for all $c \in [K]$.

Under our model assumption, given the nodes S_j and R_j, and the corresponding cluster labels, the interaction E_j is a Bernoulli random variable, with $\mathbb{E}(E_j)$ being specified by $C_j^{(s)}$ and $C_j^{(r)}$, denoted as $\mathbb{E}(E_j) = \mathcal{B}(C_j^{(s)}, C_j^{(r)})$, where $\mathcal{B}$ is a $K \times K$ propensity matrix. In the remainder of this paper, $\mathcal{B}(c,)$ is used to indicate the cth row of $\mathcal{B}$, $c \in [K]$.

2.3 Sequential description of the C-VCM model

We next provide a sequential description of a particular family of relatively exchangeable interaction processes. For ease of comprehension, the process is described in the context of TalkLife posts assuming a single commentator. Suppose m posts $E_{[m]} := \{E_1, ..., E_m\}$ have been observed along with the cluster assignments for each observed individual. That is, the post $j \in [m]$ is given by $E_j = (\{S_j, C_j^{(s)}\}, \{R_j, C_j^{(r)}\})$ where S_j is the sender and R_j is the commentator, $S_j, R_j \in \mathbb{N}$, and the cluster assignments are given by $C_j^{(s)}$ and $C_j^{(r)}$, where $C_j^{(s)}$ and $C_j^{(r)} \in [K]$. Let $\mathcal{H}_m^{(c)}$ denote the set of unique individuals in cluster $c \in [K]$ that have either posted or commented on a post in the first m interactions.

The next post, E_{m+1}, conditional on $E_{[m]}$ and the associated cluster assignments are constructed by first drawing a cluster, denoted $C_{m+1}^{(s)}$, according to

$$P(C_{m+1}^{(s)} = c|\pi_1, ..., \pi_K) = \pi_c, \text{ for } c \in [K] \tag{1}$$

where π_c is the pre-specified propensity of an interaction initiated from the cluster c, such that $\sum_{c=1}^{K} \pi_c = 1$. Note that each individual per cluster can be involved in multiple interactions, either as a poster or commentator. Let $D_m(i, c)$ be the number of times individual $i \in \mathcal{H}_m^{(c)}$ in cluster c has been observed (either has poster or commentator) in the first m interactions. Similar to the Chinese Restaurant Process [16], given parameters $0 < \alpha_c < 1$ and $\theta_c > -\alpha_c$ for each $c \in [K]$, poster S_{m+1} can be either chosen from one of the previously observed nodes i in cluster c, or an unobserved node in cluster c with probability:

$$P(S_{m+1} = s \mid \mathcal{H}_m, C_{m+1}^{(s)} = c) \propto \begin{cases} D_m(i, c) - \alpha_c, & \text{if } s = i \in \mathcal{H}_m^{(c)} \\ \theta_c + \alpha_c \sum_{i \in \mathcal{H}_m^{(c)}} D_m(i, c), & \text{if } s \notin \mathcal{H}_m^{(c)} \end{cases} \tag{2}$$

Given the sender, a similar process is used to choose the $(m+1)st$ commentator. Suppose the within and between cluster propensity of link is known. That is, the entries in the propensity matrix $\mathcal{B}$ are given. The cluster assignment for R_{m+1}, denoted $c' = C_{m+1}^{(r)} \in [K]$, is given by:

$$P(C_{m+1}^{(r)} = c'|C_{m+1}^{(s)} = c, \mathcal{B}) = \mathcal{B}(c, c')$$

Let the set of previously observed nodes in cluster c' in the first m interactions be $\mathcal{H}_m^{(c')}$. Note that if $c' = c$, $\mathcal{H}_m^{(c')} = \mathcal{H}_m^{(c')} \cup \{s\}$, and $D_m(s, c') = D_m(s, c') + 1$. Let R_{m+1} be the commentator of the $(m+1)$st interaction. Similar to the process of selecting the sender S_{m+1}, conditional on $\mathcal{H}_m^{(c')}$, the receiver node R_{m+1} is selected with probability whose explicit form is similar to that of Eq. 2

Let $\mathbf{C}_m$ denote the cluster assignments of all observed nodes in the first m interactions. Based on the above sequential description, given the total number of observed interactions being m, the proposed cluster exchangeable interaction process (C-VCM) takes the explicit form:

$$P(\mathcal{Y}_m = \mathbf{y}_m | \{\alpha_c, \theta_c\}, \mathbf{C}_m) = \underbrace{\prod_{c=1}^{K} \pi_c^{L_c}}_{(I)} \times \underbrace{\frac{[\alpha_c + \theta_c]_{\alpha_c}^{v(\mathbf{y}_c)-1}}{[\theta_c + 1]_1^{m(\mathbf{y}_c)-1}} \prod_{j \in \mathcal{H}_m^{(c)}} [1 - \alpha_c]_1^{D_m(j,c)-1}}_{(II)} \times \underbrace{\prod_{c'=1}^{K} \mathcal{B}(c, c')^{W_m(c,c')}}_{(III)} \tag{3}$$

where L_c is the number of observed interactions that are initiated from cluster c; $W_m(c, c')$ is the number of observed interactions from cluster c to c'. Part (I) of Eq. 3 is the probability of an interaction initiating from cluster c. Part (II) of Eq. 3 is the joint distribution of all the nodes within the same cluster $\mathcal{H}_m^{(c)}$ which can be expressed explicitly as [16]: $P(\mathcal{H}_m^{(c)} | \alpha_c, \theta_c, \{C_m\}) = \frac{[\alpha_c+\theta_c]_{\alpha_c}^{v(\mathbf{y}_c)-1}}{[\theta_c+1]_1^{m(\mathbf{y}_c)-1}} \prod_{j \in \mathcal{H}_m^{(c)}} [1 - \alpha_c]_1^{D_m(j,c)-1}$, where for real number x and a, and non-negative integer N, the operation on x, $[x]_a^N = x(x + a)...(x + (N - 1)a)$. Part (III) of Eq. 3 is the propensity of connection between cluster c and c'.

2.4 Statistical Properties

Given the sparsity of the network is highlighted in our model, one of the key issues to be addressed is whether the sparsity holds in both the sub-networks and the entire network. With the presence of the latent community structure, we argue that for the mixture of sub-networks following the power-law distributions parameterized by different values, the overall sparsity still holds in the entire network with minor restrictions on the propensity matrix.

Theorem 2.4 (Sparsity) *Let K be the number of clusters in the graph, such that $\forall\ c \in [K]$:*

$$\limsup_{m(\mathcal{Y}_c)\to\infty} \frac{m(\mathcal{Y}_c)}{v(\mathcal{Y}_c)^2} = 0$$

That is, the sparsity in each sub-network. Let a and b denote the diagonal and off-diagonal elements of the propensity matrix. Assume p and q are the same across clusters, and $a = \mu K b$ $(a > b)$, where μ is a normalizing constant that doesn't change with respect to the number of clusters, then

$$\limsup_{m(\mathcal{Y}_m)\to\infty} \frac{m(\mathcal{Y}_m)}{v(\mathcal{Y}_m)^2} = 0$$

That is, the overall sparsity of the entire network.

The proof can be found in Appendix 6.2. Another important question in the community detection is whether the latent community structure can be recovered. The theoretical guarantee of the various implementations of SBM and DCSBM has been well established. For example, the general theory for checking consistency of community detection under DCSBM and SBM and the comparison of several criteria are shown in [28]; the minimax optimal rate of community detection is discussed in ([7], [6]). Here, we follow the logic of proof as shown in the pseudo-likelihood methods for community detection [2] and show that as the total degrees of network increases, the mis-specification rate will be bounded.

Theorem 2.5 (Consistency) *Given the power-law parameters α_c and θ_c for all $c \in [K]$, let $v(\mathcal{Y}_m)$ be the number of nodes in the network; $m(\mathcal{Y}_m)$ be the total degree of the graph; and $\gamma m(\mathcal{Y}_m)$ be the exactly number of node in community 1 under the labeling e of all the possible permutations. Assume there are two underlying clusters in the network and $\alpha_1 = \alpha_2$ and $\theta_1 = \theta_2$.*

Let $h(\gamma)$ be the binary entropy function of γ and $\kappa_\gamma(n) = \frac{1}{n}[\log \frac{n}{4\pi\gamma(1-\gamma)} + \frac{1}{3n}]$. Denote $M_{v(\mathcal{Y}_m)} = \frac{1}{v(\mathcal{Y}_c)} \sum_{i=1}^{v(\mathcal{Y}_c)} 1(\hat{C}^{(i)} \neq C^{(i)})$. Then, as $m(\mathcal{Y}_m) \to \infty$, for a sequence $\mu_n \geq \frac{1}{e}$, we have:

$$\mathbb{P}[\sup_e M_{v(\mathcal{Y}_m)} \geq \frac{4h(\gamma)}{\log \mu_n}] \leq \exp\left[-2v(\mathcal{Y}_m)(h(\gamma) - \kappa_\gamma(2v(\mathcal{Y}_m))\right]$$

where $\hat{C}^{(i)}$ and $C^{(i)}$ stands for the inferred cluster assignment of the node i in the network and the underlying truth.

Note on the right hand side, the bound will $\to 0$ as the observations increase. The boundary value $\frac{h(\gamma)}{\log \mu_n}$ on the left hand side, as a function of γ, forms an inverted U-shape curve as γ goes from 0 to 1. See Appendix 6.1 for the proof and the discussion of the boundary values.

3 Inference

In this section, we are going to demonstrate the efficacy of our algorithm regarding the inference of network structures. We start with a brief introduction of the inference algorithm, and proceed into the accurate estimate of the power-law parameters and the recoverability of the cluster assignment. At the end of this section, we propose one potential model selection criteria based on the marginal log likelihood.

3.1 A Gibbs-sampling based inferential algorithm

Unfortunately, the likelihood shown in Eq.3 does not have closed form solutions for the parameters $\{\alpha_c\}$, $\{\theta_c\}$, and $\{\mathbf{C}_m\}$. Here, we present a Bayesian approach to infer these model parameters. We start with the selection of the priors. First, consider the cluster assignment $\mathbf{C}_m$. Recall that the probability of an interaction initiating from a specific cluster is given by π. Here, we assume a Dirichlet prior on pi, such that $\pi \sim \text{Dirichlet}(\eta)$. Without strong prior information, we'd suggest η being a symmetric Dirichlet.

As of the connection between and within the cluster, a node has to be connected to another node either in the same cluster or in the other cluster. Hence, the entries in the same row of propensity matrix $\mathcal{B}$ should sum up to 1. Without forcing the propensity matrix to be symmetric, we proposed here a row-wise Dirichlet prior, such that $\text{P(B(c,}\cdot\text{))} \sim \text{Dirichlet}(\nu),\ c \in [K]$

In terms of the priors of power-law parameters $\{\alpha_c\}$ and $\{\theta_c\}$, let $\alpha_c \sim P(\mu)$, $\theta_c \sim P(\delta)$, $c \in [K]$. A reasonable choice could be the Beta distribution and the Gamma distribution correspondingly such that the posterior distribution will have the close form to sample from.

Given the specified priors, we introduce the algorithm built upon Gibbs sampling to infer the model parameters. Based on the description of our model, the parameters to be updated are the power-law parameters $\{\alpha_c\}$, $\{\theta_c\}$, and the latent clustering assignment indicator $\{\mathbf{C}_m\}$. The

description of the algorithm is shown as follows:

Algorithm 1 Pseudo-code of Gibbs-sampling based algorithm

```
Specify η, ν, σ, μ, K
Initiate ℬ, {α_c}, {θ_c}, {C_m}
for iterations do
    for s ∈ v(𝒴_m) do
        Update C_m^(s) according to Eq (4)
    end for
    for c ∈ [K] do
        Update α_c according to Eq (6)
        Update θ_c according to Eq (5)
    end for
    for c ∈ [K] do
        Update ℬ(c, ) from the Dirichlet distribution
    end for
end for
```

The first parameter to be updated is $\{\mathbf{C}_m\}$. The conditional updates of latent cluster indicator $\{\mathbf{C}_m\}$ is based on the following derivations. Suppose the algorithm is assigning a specific node $s \in \{\mathcal{H}_m\}$ to a specific cluster $c \in \{1, ..., K\}$. The corresponding probability p_c is proportional to:

$$p_c \propto \underbrace{P(\{C_m^{(s)}\} = c|\eta)}_{(I)} \times \underbrace{P(\mathcal{B}(C_m^{(s)} = c,)|\nu)}_{(II)} \times \underbrace{P(\{\mathcal{H}_m^{(c)}\}|\alpha_c, \theta_c, \delta, \mu)}_{(III)}$$

The first term (I) can be achieved through integrating the latent parameter π from $P(\{C_m^{(s)}\}|\pi, \eta)$ in a way that

$$P(\{C_m^{(s)}\}|\eta) = \int_\pi P(\{C_m^{(s)}\}|\pi)P(\pi|\eta)d\pi = \frac{\mathscr{B}(\eta + L)}{\mathscr{B}(\eta)}$$

where $L = \{L_1, ..., L_K\}$ is the counts of the interactions initiated from cluster 1 to K, and $\mathscr{B}(\cdot)$ is the Beta function.

The second term II can be simplified by considering only the nodes that have connections with the node s that is updated in the current iteration. Let $D_m(s, c)$ be the degree of node s, and $D_m(s, 1)$ to $D_m(s, K)$ be the number of interactions node s has with nodes in cluster 1 to K

correspondingly:

$$P(\mathcal{B}(C_m^{(s)}=c,)|\nu) \propto \frac{D_m(s,c)!}{D_m(s,1)!...,D_m(s,K)!}\prod_{c'=1}^{K}\mathcal{B}(c,c')^{D_m(s,c')}$$

The third term III takes the explicit form as shown in Eq (4). Normalizing over different p_c over $c \in [K]$, we get the conditional probability of assigning the node to cluster c:

$$P(C_m^{(s)}=c|\alpha_c,\theta_c,B,\eta,\mu,\delta) \sim \text{Multinomial}(\frac{p_c}{\sum_{k=1}^{K}p_k}) \tag{4}$$

The conditional updates of α_c and θ_c is shown as follows. Given the cluster allocation $\{\mathbf{C}_m\}$, the values of α_c and θ_c can be sampled from the posterior distribution. First, consider the θ_c:

$$P(\theta_c|\{\mathbf{C}_m\},\delta) \propto \frac{[\theta_c+\alpha_c]_{\alpha_c}^{v(\mathbf{y}_c)-1}}{[\theta_c+1]_1^{m(\mathbf{y}_c)-1}}P(\theta_c|\delta)$$

Here, we utilize a similar idea of sampling auxiliary variable methods [23] that was also introduced in the hierarchical e2 model [5]. Let $\{\alpha_c^*\}$ and $\{\theta_c^*\}$ be the values of the power-law parameters from the previous Gibbs updating iteration, and $\{a,b,c,d\}$ be the pre-specified constants. Then, the denominator of the above equation can be written as $([\theta_c+1]^{m(\mathbf{y}_c)-1})^{-1} = \Gamma(m(\mathbf{y}_c)-1)^{-1}\int_0^1 x^{\theta_c}(1-x)^{m(\mathbf{y}_c)-2}dx$, where x is an intermediate variable that can be sampled given $\{\theta_c^*\}$, such that $x \sim Beta(\theta_{c^*}+1, m(\mathbf{y}_c)-1)$. Similarly, the nominator $[\theta_c+\alpha_c]_{\alpha_c}^{v(\mathbf{y}_c)-1} = \prod_{i=1}^{v(\mathbf{y}_c)-1}\sum_{y_i\in[0,1]}\theta_c^{y_i}(\alpha_c*i)^{1-y_i}$ where $y_i \sim Bernoulli(\frac{\theta_c^*}{\theta_c^*+\alpha_c^**i})$. Eventually, the posterior of θ_c is given by

$$\theta_c|C_m \sim \text{Gamma}(\sum_{i=1}^{v(\mathbf{y}_c)-1} y_i + a, b - logx) \tag{5}$$

.

Similarly, the posterior of α_c is given by

$$\alpha_c|C_m \sim \text{Beta}(c+\sum_{i=1}^{v(\mathbf{y}_c)-1}(1-y_i), d+\sum_{s_c}\sum_{j=1}^{D_m(c,s)-1}(1-z_{s_c,j})) \tag{6}$$

where $y_i \sim \text{Bernoulli}(\frac{\theta_c}{\theta_c+\alpha_c*i})$ and $z_{s_c,j} \sim \text{Bernoulli}(\frac{j-1}{j-\alpha_c^*})$.

To summarize, the algorithm first draws the values of intermediate variables x, y, and z based

on the previous round values of α_c^* and θ_c^*. Given the values of these variables, we draw the values of the updated α_c and θ_c according to Eq.5 and Eq.6.

Last but not least, given the cluster allocation $c \in [K]$, the row-wise update of the propensity matrix will be from the Dirichlet distribution given the prior.

3.2 Power-law parameter inference

An important question is whether the posterior distributions adequately concentrate around the true cluster-specific parameters $\{\alpha_c\}_{c\in[K]}$ which controls the within-cluster sparsity and power-law structure. Here, a generative model as described in Section 2.3 is used to simulate various networks to assess our ability to accurately estimate these parameters.

Here we focus on simulations where the number of clusters K is equal to 2. In this setting, we choose $\{\alpha_1, \alpha_2\}$ from $\{\{0.1, 0.9\}, \{0.2, 0.8\}, \{0.3, 0.7\}, \{0.4, 0.6\}\}$ and set $\theta_1 = \theta_2 = 5$. The within-group interaction propensity is set to 0.9 (i.e., $a := \mathcal{B}(1,1) = \mathcal{B}(2,2) = 0.9$), and between-group is set to 0.1 (i.e., $b := \mathcal{B}(1,2) = \mathcal{B}(2,1) = 0.1$). Clusters are assumed equally likely to initiate an interaction (i.e., $\{\pi_1, \pi_2\} = \{0.5, 0.5\}$). Networks of size 1,000, 10,000 and 100,000 were simulated, repeated 20 times. Given the priors specified in the previous section, the means of the posterior of the power-law parameters and the entries in propensity matrix are shown in Table 1. The results are shown in Table 1.

First, estimation accuracy is higher when the networks are more loosely connected. For example, in the 1000 interactions setting where $\{\alpha_1, \alpha_2\} = \{0.3, 0.7\}$, the power-law estimates when the truth is equal to 0.7 are more accurate than the estimates when the truth is equal to 0.3. Second, power-law estimation accuracy degrades as the inter-community connection rate increases. For example, in the 1000 interaction setting where $\{\alpha_1, \alpha_2\} = \{0.2, 0.8\}$, the power-law estimate decreases in accuracy as the likelihood of inter-community connections goes up from 0.1 to 0.5. Third, estimation accuracy increases as the number of interactions increase. For example, in the case where $\alpha_1 = 0.1$, and $\{a, b\} = \{0.9, 0.1\}$, the power-law estimate becomes more accurate as the sample size grows from $N = 1,000$ to $100,000$.

3.3 Recovering Cluster Assignment Labels

We show in Theorem 2.5 the mis-specification rate of C-VCM can be bounded. Here, we show in simulation that the posterior concentrates on the correct cluster assignment labels. The same simulation settings are inherited from the previous section, and are used to empirically confirm the ability of our algorithm to recover the underlying network structure when only a finite number of interactions are observed. The cross entropy loss is used to measure the misclassification loss. We start by defining the cross entropy loss for a specific cluster $c \in [K]$:

$$\mathscr{L}_c = \sum_{j \in \mathcal{H}_m^{(c)}} -p(C_j = c) \log q(\hat{C}_j = c)$$

where the $p(\cdot)$ is the true cluster assignment, and $q(\cdot)$ is the posterior mean of the inferred cluster assignment. Further define the average per node entropy loss $\mathscr{L}_s = \frac{1}{v(y_m)} \sum_{c=1}^{K} \mathscr{L}_c$,

The results are shown in Table 2. First, for fixed $\{\alpha_1, \alpha_2\}$, the higher the within cluster connection probability, the better the recovery of the cluster assignments. Second, as the number of observations increases, the cluster assignments become more accurate in almost all settings. Third, fix {a,b}, as the difference in power-law parameters decreases between the two clusters, the cluster assignment accuracy decreases.

3.4 The selection of K

So far, we have assumed K is known and set to be 2. It remains to be addressed the selection of K. The well-acknowledged solutions include but are not limited to the likelihood ratio test based methods ([25], [26]), the cross validation based methods ([9],[8]), and the Bayesian selection criteria ([27],[22]). Though proven to be a big success in many cases, these methods cannot fit into our settings well. The likelihood ratio test based method requires a good distributional approximation, which is hard to find in our setting; and cross validation based methods bring the even more complex sampling issues and the lack of the interpretation; and the implementation of Bayesian selection criteria can be very computationally expensive.

Here, we consider a model selection criteria based on the marginal posterior maximization that

is similar to the one used in the topic models[21]. Based on this criteria, the number of clusters is determined by choosing the K that gives the largest marginal likelihood $P(\mathbf{y}_m|\{\alpha_c, \theta_c\}, \mathbf{C}_m, K)$. Simulation results show solid support to our proposed method (Appendix 6.4). Future work is required for a formal study of the model selection criteria in the cluster edge exchangeable model.

4 Case Study

4.1 Data overview

In this section, we apply the C-VCM to the TalkLife dataset which consists of millions of user posts and comments. Here we consider all non-deleted posts on TalkLife during the year 2019, consisting of 1,508,895 posts with an average of 2.82 comments per post, leading to 4,258,792 post-comment pairs. TalkLife deploys a series of classification algorithms to flag posts if they include language related to one of several mental health topics. For example, a post can be flagged as *Anxiety Panic Fear Suspected* if the corresponding classifier was triggered by the text of the post. There are a total of 33 classifiers applied to the majority of posts. Figure 2 shows the global degree distribution for posts, and the degree distribution for posts flagged by 4 out of 33 different classifiers

4.2 Inferring Cluster labels

In this section, we aim to identify the latent community structure of TalkLife users. In the running example shown in Section 2.2, the model only considers pairs where each user only compose a single poster. In TalkLife, however, the data consists of multiple posters posted by a singe user. Here, we make an independence assumption of different posters posted by the same user.

In the following analysis, we focus on users that pay attention to posts of similar themes. We subset the data based on these machine learning generated tags. Given the network built from posts with a particular machine learning tag, we run the Gibbs-sampling algorithm to learn the latent community structure. We consider a varying number of clusters and infer the cluster assignments of each user over a range of K values.

We further investigate the within and the between cluster connectivity of the inferred commu-

nities. Using Alcohol and Substance Abuse network as an example, the count of the interactions when K is set to be 2, 6, and 10 is shown in Figure 3. It is consistently witnessed that the within community connectivity is greater than the between community connectivity based on the results of our method, which indicates the existence of the clustering structures of the users.

4.3 Comparison with Spectral Clustering

In the section, we further compare our method with the spectral clustering method ([24],[14]). To implement the spectral clustering method, we construct a binary graph. The connectivity of the communities detected by the spectral clustering method in Alcohol and Substance Abuse network is shown in Figure 3. The spectral clustering method gives different community structures as compared to our method. Also note there is little variations in the nodes clustered to the largest two groups by spectral clustering over different K values. This makes the communities detected by the spectral clustering method less informative than our method.

To further assess the quality of the inferred latent community structure, we check the consistency of the clusters inferred by our algorithm over time. We split the data into two halves based on whether the post occurred before June 30th, and infer the latent community structure within each time window using our proposed approach and spectral clustering. The Hellinger distance is used to quantify the difference between the cluster assignments, which is defined as:

$$HL = \frac{1}{v(\mathbb{Y}_m)} \sum_{i=1}^{v(\mathbb{Y}_m)} \frac{1}{\sqrt{2}} \sqrt{\sum_{k=1}^{K} (\sqrt{p_{ki}} - \sqrt{q_{ki}})^2}$$

where p and q correspond to the probability of a node belonging to one of the Kth clusters given by the Gibbs iterations and the underlying truth. To address the label switching problem, we take the minimal Hellinger distance as the final one.

For illustrative purposes, we use the *Alcohol and Substance Abuse Suspected* and *Behavioral Symptoms Suspected* networks as our two running examples. (See more modeling fitting results in different sub-networks in Appendix 6.5.) The results are shown in Figure 4. Due to uncertainty in K, we look at a range of values. In the Behavioral Symptoms Suspected network, the marginal likelihood $P(\mathbf{Y}|m|K, \{\alpha_c\}, \{\theta_c\}, \mathbb{C}_m)$ hits the largest value when $K = 4$, which indicates setting the

underlying communities to be 4 is the most reasonable grouping of users. In the both networks, the Hellinger Distance of clustering assignments of our model is consistent with the marginal likelihoods. It serves to prove the efficacy of the heuristic strategy mentioned in Section 3.4 in real data.

When compaing to the spectral clustering methods, the minimal Hellinger Distance of the cluster assignment is smaller in our model, which indicates the communities detected by our method are more consistent over time than the communities detected by the spectral clustering method. That is, users tend to have more connections with people from the same inferred communities than people outside the inferred communities over time.

5 Discussion

In this paper, we have proposed a new method that can be applied to cluster the nodes and identify the underlying community structures of real world networks. Specifically, our method features modeling the network from the interaction process perspective and incorporating the power-law property which is observed in many large sparse networks. We demonstrate the efficacy of our algorithm through simulation and finalize this paper by applying our method to the TalkLife data to identify the potential online user communities.

The contribution of our work is to account for the community structure when modeling the interaction process. Using TalkLife data as an example, our method can identify the underlying users' groups so that the platform will know to whom they can boost the visibility of the posts from certain users. Besides, our method provides the estimates of the power-law parameters for each of the group. The revelation of the network properties can help the platform make proper decisions on what kind of interventions to make. For example, a smaller power-law parameter indicates a looser connection between users. The platform will need extra efforts to ensure certain users within the community getting enough attention and social supports. Though we demonstrate our method using the TalkLife data, it can be well applied to any sparse interaction data sets [19].

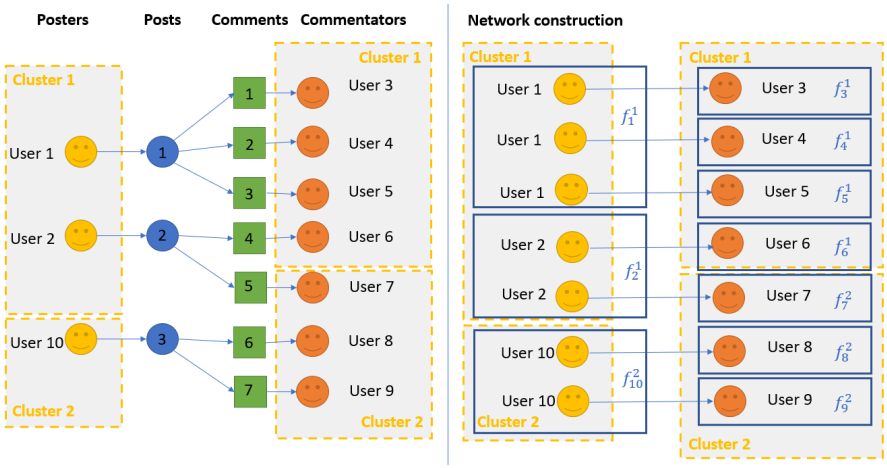

Figure 1: Interaction data collected on TalkLife (Left), and the corresponding network (Right). In this example, there are 3 posts and 10 users involved. Post 1 posted by User 1, is commented by User 3, 4, and 5; Post 2 posted by User 2 is commented by User 6 and 7; Post 3 posted by User 10 is commented by User 8 and 9. The network is constructed by connecting User 1 to User 3, 4, and 5; User 2 to User 6 and 7; User 10 to User 8 and 9. Note that User 1, 2, 3, 4, 5, 6 are from cluster 1, and the rest users are from cluster 2. Therefore, 4 of the interactions are from cluster 1 to cluster 1, 1 of them is from cluster 1 to cluster 2, the rest are from cluster 2 to cluster 2.

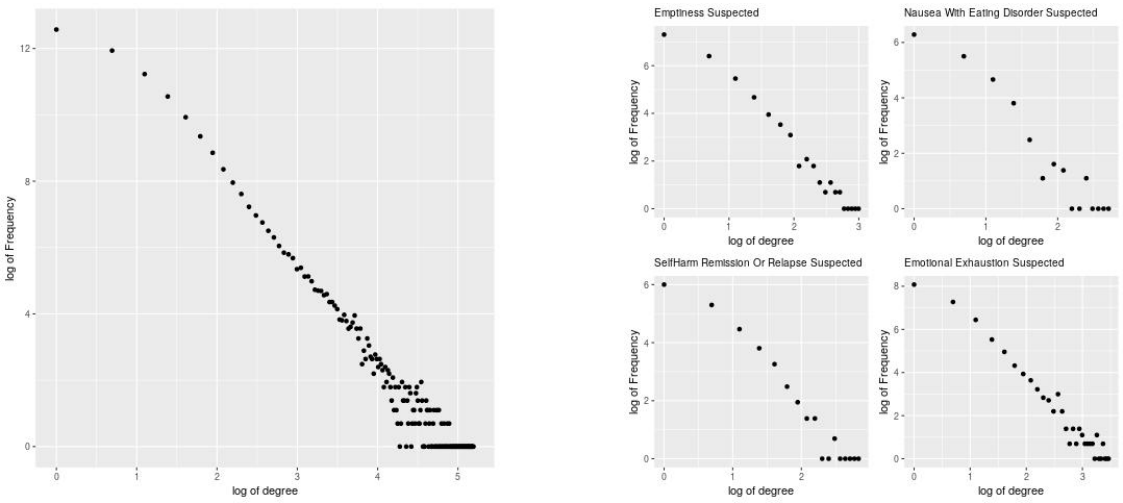

(a) Overall degree plot of 2019 senders (b) Degree plot of 2019 senders by different tags

Figure 2: (a) Overview of the degree distribution of 2019 senders; (b) Degree distribution of the 2019 senders in sub-networks The power-law degree distribution is observed in all the networks.

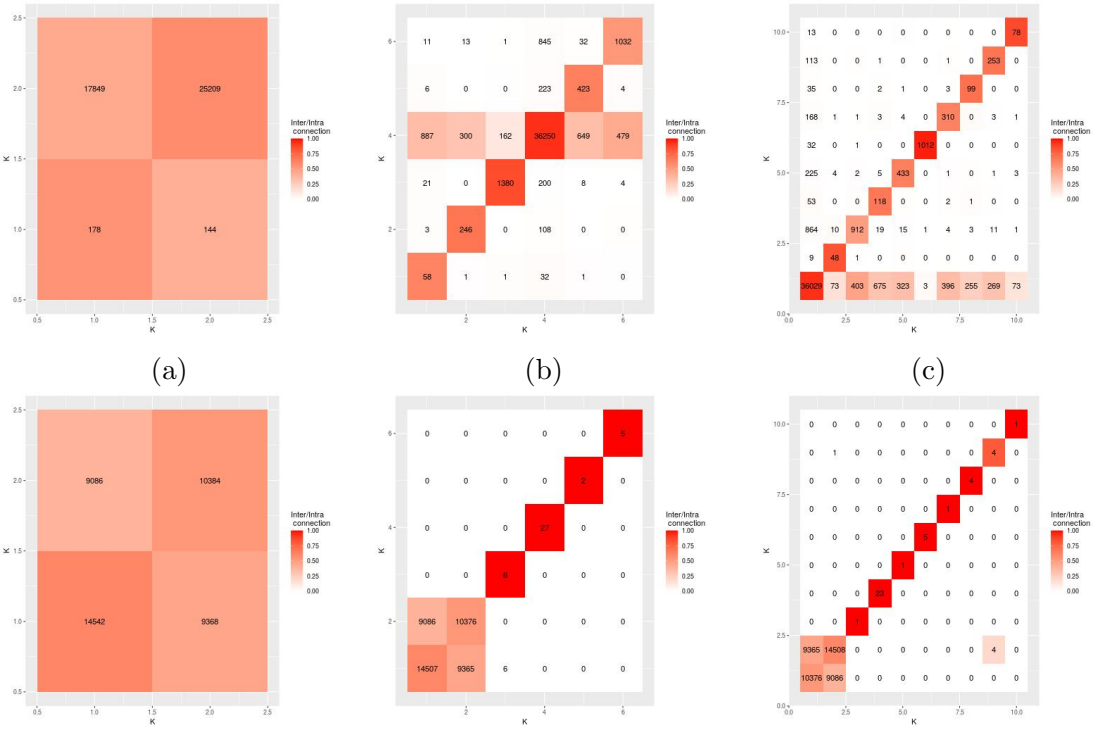

(a) (b) (c)

(d) (e) (f)

Figure 3: The inter/intra connectivity of the communities detected by our algorithm ((a)(b)(c)) and the spectral clustering ((d)(e)(f)), ranging from 0 to 1, indicating the proportion of the interactions that initiated fro one cluster to the other. The number within each cell is the count of the directed interactions.

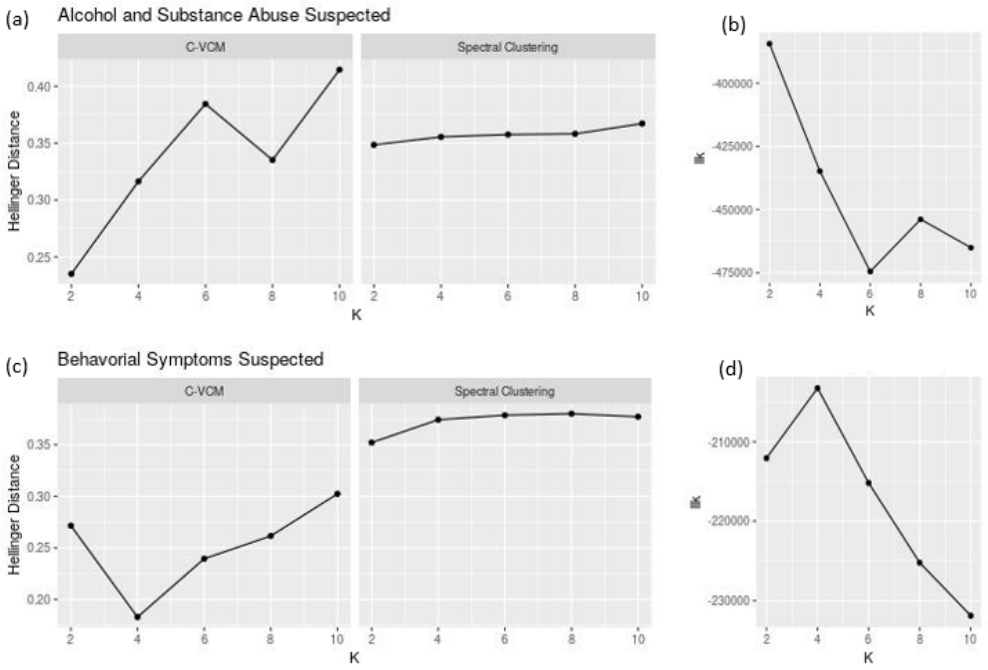

Figure 4: The Hellinger distances of the cluster assignment between the first half and the second half of the 2019 data in (a) Alcohol and Substance Abuse suspected network and (c) Behavorial Symptoms Suspected network. The marginal likelihood over different K values in (b) Alcohol and Substance Abuse suspected network and (d) Behavorial Symptoms Suspected network.

1,000 interactions	Parameters	$\{\alpha_c\} = \{0.1, 0.9\}$	$\{\alpha_c\} = \{0.2, 0.8\}$	$\{\alpha_c\} = \{0.3, 0.7\}$	$\{\alpha_c\} = \{0.4, 0.6\}$
$\{a, b\} = \{0.9, 0.1\}$	α_1	**0.301 (0.182)**	**0.296 (0.116)**	**0.374 (0.08)**	**0.449 (0.083)**
	$\tilde{\alpha}_1$	0.200 (0.100)	0.274 (0.084)	0.354 (0.068)	0.460 (0.086)
	α_2	**0.886 (0.079)**	**0.804 (0.022)**	**0.712 (0.037)**	**0.612 (0.056)**
	$\tilde{\alpha}_2$	0.904 (0.015)	0.805 (0.021)	0.714 (0.037)	0.604 (0.057)
	Diagonal	0.907 (0.020)	0.905 (0.019)	0.903 (0.019)	0.898 (0.018)
$\{a, b\} = \{0.7, 0.3\}$	α_1	**0.335 (0.196)**	**0.335 (0.139)**	**0.412 (0.143)**	**0.501 (0.099)**
	$\tilde{\alpha}_1$	0.226 (0.094)	0.256 (0.095)	0.384 (0.113)	0.470 (0.100)
	α_2	**0.886 (0.069)**	**0.801 (0.029)**	**0.704 (0.061)**	**0.604 (0.064)**
	$\tilde{\alpha}_2$	0.901 (0.015)	0.806 (0.025)	0.712 (0.061)	0.617 (0.058)
	Diagonal	0.709 (0.031)	0.710 (0.028)	0.708 (0.030)	0.708 (0.034)
$\{a, b\} = \{0.5, 0.5\}$	α_1	**0.627 (0.162)**	**0.624 (0.185)**	**0.613 (0.115)**	**0.523 (0.124)**
	$\tilde{\alpha}_1$	0.212 (0.096)	0.290 (0.079)	0.368 (0.078)	0.479 (0.105)
	α_2	**0.800 (0.267)**	**0.726 (0.125)**	**0.604 (0.112)**	**0.555 (0.106)**
	$\tilde{\alpha}_2$	0.898 (0.017)	0.804 (0.025)	0.710 (0.030)	0.601 (0.064)
	Diagonal	0.521 (0.042)	0.532 (0.051)	0.540 (0.053)	0.526 (0.050)
10,000 interactions	Parameters	$\{\alpha_c\} = \{0.1, 0.9\}$	$\{\alpha_c\} = \{0.2, 0.8\}$	$\{\alpha_c\} = \{0.3, 0.7\}$	$\{\alpha_c\} = \{0.4, 0.6\}$
$\{a, b\} = \{0.9, 0.1\}$	α_1	**0.201 (0.089)**	**0.273 (0.083)**	**0.336 (0.051)**	**0.426 (0.042)**
	$\tilde{\alpha}_1$	0.175 (0.063)	0.244 (0.063)	0.336 (0.043)	0.420 (0.039)
	α_2	**0.899 (0.006)**	**0.799 (0.011)**	**0.700 (0.017)**	**0.605 (0.020)**
	$\tilde{\alpha}_2$	0.900 (0.006)	0.800 (0.011)	0.701 (0.017)	0.607 (0.019)
	Diagonal	0.900 (0.006)	0.900 (0.006)	0.901 (0.006)	0.900 (0.006)
100,000 interactions	Parameters	$\{\alpha_c\} = \{0.1, 0.9\}$	$\{\alpha_c\} = \{0.2, 0.8\}$	$\{\alpha_c\} = \{0.3, 0.7\}$	$\{\alpha_c\} = \{0.4, 0.6\}$
$\{a, b\} = \{0.9, 0.1\}$	α_1	**0.157 (0.063)**	**0.242 (0.054)**	**0.322 (0.034)**	**0.413 (0.025)**
	$\tilde{\alpha}_1$	0.136 (0.045)	0.220 (0.040)	0.319 (0.027)	0.412 (0.022)
	α_2	**0.900 (0.002)**	**0.799 (0.004)**	**0.700 (0.006)**	**0.604 (0.012)**
	$\tilde{\alpha}_2$	0.900 (0.002)	0.799 (0.004)	0.700 (0.006)	0.605 (0.011)
	Diagonal	0.900 (0.002)	0.900 (0.002)	0.900 (0.002)	0.900 (0.002)

Table 1: Posterior means (SD) of power-law parameters $\{\alpha_c\}$ and within/between cluster propensity $\{a, b\}$ in different settings. To assess uncertainty due to latent communities, we also infer the posteriors of power-law parameters given true cluster assignments, denoted $\tilde{\alpha}_c$, $c \in [K]$. Three main conclusions are highlighted in red, yellow, and blue correspondingly.

	Interactions	$\{\alpha_c\} = \{0.1, 0.9\}$	$\{\alpha_c\} = \{0.2, 0.8\}$	$\{\alpha_c\} = \{0.3, 0.7\}$	$\{\alpha_c\} = \{0.4, 0.6\}$
$\{a, b\} = \{0.1, 0.9\}$	1,000	0.056 (0.014)	0.095 (0.028)	0.152 (0.028)	0.212 (0.040)
	10,000	0.014 (0.004)	0.039 (0.013)	0.094 (0.012)	0.170 (0.032)
	100,000	0.0027 (0.0006)	0.013 (0.004)	0.054 (0.012)	0.134 (0.018)
$\{a, b\} = \{0.2, 0.8\}$	1,000	0.084 (0.020)	0.151 (0.032)	0.239 (0.065)	0.343 (0.050)
	10,000	0.019 (0.005)	0.055 (0.015)	0.157 (0.084)	0.298 (0.074)
	100,000	0.013 (0.033)	0.018 (0.004)	0.097 (0.040)	0.223 (0.029)
$\{a, b\} = \{0.3, 0.7\}$	1,000	0.102 (0.152)	0.182 (0.050)	0.346 (0.100)	0.445 (0.061)
	10,000	0.052 (0.118)	0.078 (0.020)	0.210 (0.089)	0.411 (0.123)
	100,000	0.039 (0.086)	0.048 (0.060)	0.099 (0.016)	0.342 (0.124)
$\{a, b\} = \{0.4, 0.6\}$	1,000	0.161 (0.082)	0.345 (0.117)	0.489 (0.097)	0.625 (0.057)
	10,000	0.120 (0.129)	0.279 (0.186)	0.311 (0.120)	0.546 (0.098)
	100,000	0.291 (0.202)	0.120 (0.125)	0.216 (0.118)	0.508 (0.103)
$\{a, b\} = \{0.5, 0.5\}$	1,000	0.311 (0.202)	0.517 (0.110)	0.621 (0.052)	0.658 (0.067)
	10,000	0.254 (0.158)	0.291 (0.140)	0.434 (0.115)	0.711 (0.136)
	100,000	0.422 (0.107)	0.283 (0.146)	0.332 (0.140)	0.604 (0.049)

Table 2: Cross Entropy Loss averaged by number of nodes in different settings. For each set with the same values of the connectivity propensity $\{a, b\}$, the power-law parameters $\{\alpha_1, \alpha_2\}$, and the number of interactions ($\{1,000, 10,000, 100,000\}$), we repeated the simulation 20 times. The mean values (SD) over 20 simulations are shown here. We do observe some instability when the propensity of connection is close to 0.5 (highlighted in blue)

References

[1] Lada A Adamic et al. "Search in power-law networks". In: *Physical review E* 64.4 (2001), p. 046135.

[2] Arash A Amini et al. "Pseudo-likelihood methods for community detection in large sparse networks". In: *The Annals of Statistics* 41.4 (2013), pp. 2097–2122.

[3] Peter Chin, Anup Rao, and Van Vu. "Stochastic block model and community detection in sparse graphs: A spectral algorithm with optimal rate of recovery". In: *Conference on Learning Theory*. PMLR. 2015, pp. 391–423.

[4] Harry Crane and Walter Dempsey. "Edge exchangeable models for network data". In: *arXiv preprint arXiv:1603.04571* (2016).

[5] Walter Dempsey, Brandon Oselio, and Alfred Hero. "Hierarchical network models for exchangeable structured interaction processes". In: *Journal of the American Statistical Association* (2021), pp. 1–18.

[6] Chao Gao, Yu Lu, and Harrison H Zhou. "Rate-optimal graphon estimation". In: *The Annals of Statistics* 43.6 (2015), pp. 2624–2652.

[7] Chao Gao et al. "Community detection in degree-corrected block models". In: *The Annals of Statistics* 46.5 (2018), pp. 2153–2185.

[8] Justin Grimmer. "A Bayesian hierarchical topic model for political texts: Measuring expressed agendas in Senate press releases". In: *Political Analysis* 18.1 (2010), pp. 1–35.

[9] Bettina Grün and Kurt Hornik. "topicmodels: An R package for fitting topic models". In: *Journal of statistical software* 40.1 (2011), pp. 1–30.

[10] Paul W Holland, Kathryn Blackmond Laskey, and Samuel Leinhardt. "Stochastic blockmodels: First steps". In: *Social networks* 5.2 (1983), pp. 109–137.

[11] Brian Karrer and Mark EJ Newman. "Stochastic blockmodels and community structure in networks". In: *Physical review E* 83.1 (2011), p. 016107.

[12] Evan M Kleiman and Richard T Liu. "Social support as a protective factor in suicide: Findings from two nationally representative samples". In: *Journal of affective disorders* 150.2 (2013), pp. 540–545.

[13] Morten Mørup and Mikkel N Schmidt. "Bayesian community detection". In: *Neural computation* 24.9 (2012), pp. 2434–2456.

[14] Andrew Y Ng, Michael I Jordan, and Yair Weiss. "On spectral clustering: Analysis and an algorithm". In: *Advances in neural information processing systems*. 2002, pp. 849–856.

[15] SL van der Pas and AW38078661407 van der Vaart. "Bayesian community detection". In: *Bayesian Analysis* 13.3 (2018), pp. 767–796.

[16] Jim Pitman et al. *Combinatorial stochastic processes*. Tech. rep. Technical Report 621, Dept. Statistics, UC Berkeley, 2002. Lecture notes for ..., 2002.

[17] Maoying Qiao et al. "Adapting stochastic block models to power-law degree distributions". In: *IEEE transactions on cybernetics* 49.2 (2018), pp. 626–637.

[18] Karl Rohe, Sourav Chatterjee, and Bin Yu. "Spectral clustering and the high-dimensional stochastic blockmodel". In: *The Annals of Statistics* 39.4 (2011), pp. 1878–1915.

[19] Piotr Sapiezynski et al. "Interaction data from the copenhagen networks study". In: *Scientific Data* 6.1 (2019), pp. 1–10.

[20] David Strauss and Michael Ikeda. "Pseudolikelihood estimation for social networks". In: *Journal of the American statistical association* 85.409 (1990), pp. 204–212.

[21] Matt Taddy. "On estimation and selection for topic models". In: *Artificial Intelligence and Statistics*. PMLR. 2012, pp. 1184–1193.

[22] Yee W Teh, David Newman, and Max Welling. *A collapsed variational Bayesian inference algorithm for latent Dirichlet allocation*. Tech. rep. CALIFORNIA UNIV IRVINE SCHOOL OF INFORMATION and COMPUTER SCIENCE, 2007.

[23] Yee Whye Teh. "A Bayesian interpretation of interpolated Kneser-Ney". In: (2006).

[24] Hadrien Van Lierde, Tommy WS Chow, and Guanrong Chen. "Scalable spectral clustering for overlapping community detection in large-scale networks". In: *IEEE Transactions on Knowledge and Data Engineering* 32.4 (2019), pp. 754–767.

[25] Quang H Vuong. "Likelihood ratio tests for model selection and non-nested hypotheses". In: *Econometrica: Journal of the Econometric Society* (1989), pp. 307–333.

[26] YX Rachel Wang and Peter J Bickel. "Likelihood-based model selection for stochastic block models". In: *The Annals of Statistics* 45.2 (2017), pp. 500–528.

[27] Xiaoran Yan. "Bayesian model selection of stochastic block models". In: *2016 IEEE/ACM International Conference on Advances in Social Networks Analysis and Mining (ASONAM)*. IEEE. 2016, pp. 323–328.

[28] Yunpeng Zhao, Elizaveta Levina, and Ji Zhu. "Consistency of community detection in networks under degree-corrected stochastic block models". In: *The Annals of Statistics* 40.4 (2012), pp. 2266–2292.

6 Appendix

6.1 Proof of Theorem 1

We follow a similar proof as shown in [2]. The overall goal of the proof is to show $\sup_e M_{v(\mathcal{Y}_m)} = \frac{1}{v(\mathcal{Y}_m)} \sum_{i=1}^{v(\mathcal{Y}_m)} 1(\hat{C}_i \neq C_i)$ is bounded. That is the probability of mis-specification of the cluster assignment goes to 0 as n goes to infinity. The likelihood in our model takes the form:

$$P(\mathcal{Y}_m = \mathbf{y}_m | \{\alpha_c, \theta_c\}, \mathbf{C}_m) = \prod_{c=1}^{K} \pi_c^{L_c} \times \frac{[\alpha_c + \theta_c]_{\alpha_c}^{v(\mathbf{y}_c)-1}}{[\theta_c + 1]_1^{m(\mathbf{y}_c)-1}} \prod_{j \in \mathcal{H}_m^{(c)}} [1 - \alpha_c]_1^{D_m(j,c)-1} \times \prod_{c'=1}^{K} \mathcal{B}(c, c')^{W_m(c,c')}$$

For simplicity of the notation, denote $(*) = \frac{[\alpha_c+\theta_c]_{\alpha_c}^{v(\mathbf{y}_c)-1}}{[\theta_c+1]_1^{m(\mathbf{y}_c)-1}} \prod_{j \in \mathcal{H}_m^{(c)}} [1 - \alpha_c]_1^{D_m(j,c)-1}$. Let $Deg(i)$ be the degree of node i, and p_i be the proportion of the interactions that are initiated from node i, and $Deg(i, 1)$ be the degree of node i being connected to nodes in cluster 1. For simplicity, let's consider two clusters scenario first. Assume $\alpha_1 = \alpha_2$ and $\theta_1 = \theta_2$, such that the log likelihood of assigning the node i to cluster 1 is:

$$l_{i,1} = (p_i * Deg(i) + L_{1,-i}) \log \pi_1 + (*) + \log[\mathcal{B}(1,1)^{W_m(1,1)} \mathcal{B}(1,2)^{W_m(1,2)}]$$

$$+ (L_{2,-i}) \log \pi_2 + (*) + \log[\mathcal{B}(2,1)^{W_m(2,1)} \mathcal{B}(2,2)^{W_m(2,2)}]$$

$$= (p_i * Deg(i) + L_{1,-i}) \log \pi_1 + (*) + [Deg(i,1) + W_{m,-i}(1,1)] \log \mathcal{B}(1,1)$$

$$+ [p_i * Deg(i,2) + W_{m,-i}(1,2)] \log \mathcal{B}(1,2)$$

$$+ (L_{2,-i}) \log \pi_2 + (*) + [(1 - p_i) * Deg(i,2) + W_{m,-i}(2,1)] \log \mathcal{B}(2,1)$$

$$+ W_{m,-i}(2,2) \log \mathcal{B}(2,2)$$

Similarly, we get $l_{i,2}$.

$$l_{i,2} = (L_{1,-i}) \log \pi_1 + (*) + [W_{m,-i}(1,1)] \log \mathcal{B}(1,1)$$

$$+ [(1 - p_i) * Deg(i,1) + W_{m,-i}(1,2)] \log \mathcal{B}(1,2)$$

$$+(p_i * Deg(i) + L_{2,-i}) \log \pi_2 + (*) + [p_i * Deg(i,1) + W_{m,-i}(2,1)] \log \mathcal{B}(2,1)$$

$$+[Deg(i,2) + W_{m,-i}(2,2)] \log \mathcal{B}(2,2)$$

Let $a = \mathcal{B}(1,1) = \mathcal{B}(2,2)$, and $b = \mathcal{B}(1,2) = \mathcal{B}(2,1)$. Thus the difference is:

$$l_{i,1} - l_{i,2} = p_i * Deg(i) * \log \frac{\pi_1}{\pi_2} + (\log a - \log b)(Deg(i,1) - Deg(i,2))$$

For simplicity, we further assume $\pi_1 = \pi_2$. Thus $\hat{c}_i = 1$ iff $Deg(i,1) > Deg(i,2)$. Assume $Deg(i,1)|Deg(i), a, b \sim$ Binomial$(Deg(i), a)$. Let $\epsilon_i = Deg(i,2) - Deg(i,1)$, thus the condition become $\epsilon_i < 0$. Define

$$N(\cdot) = \sum_{i=1}^{v(\mathcal{Y}_m)} 1(\epsilon_i \geq 0)$$

Let γ be the proportion of nodes that matches labels in community 1 under the notation system e_i. One can understand e_i as the labeling of the nodes under current Gibbs iteration. We further introduce the permutation σ of the nodes indicating whether the corresponding nodes belong to the first community, such that

$$\sum_{j=1}^{n} 1(\sigma_j = 1) = \gamma v(\mathcal{Y}_m)$$

The mis-specification rate is thus bounded by :

$$\sup_e M_{v(\mathcal{Y}_m)} \leq \sup_\sigma \frac{N(\cdot)}{v(\mathcal{Y}_m)}$$

The inequality is due to treating the ambiguous case $\epsilon_i = 0$ being an error. It is thus sufficient to show the RHS of the above inequity is bounded. We use the following steps to finish the proof.

Step 1. Using Hoeffding's inequality to show that:

$$P(\epsilon_i \geq \mathbb{E}(\epsilon_i) + t) \leq \exp[-\frac{2t^2}{Deg(i)^2}]$$

Note that

$$\mathbb{E}(\epsilon_i) = (a-b)\gamma Deg(i) + (b-a)(1-\gamma)Deg(i) = (2\gamma - 1)(a-b)Deg(i)$$

. Let $t = (1-2\gamma)(a-b)Deg(i)$ Then we have

$$P(\epsilon_i \geq 0) \leq \exp[-2(1-2\gamma)^2(a-b)^2]$$

Step 2. Show that $\frac{1}{v(\mathcal{Y}_m)}N(\cdot) = \frac{1}{v(\mathcal{Y}_m)}\sum_{i=1}^{v(\mathcal{Y}_m)} 1(\epsilon_i \geq 0)$ is bounded by something.

Note that $1(\epsilon_i \geq 0)$ is a Bernoulli random variable. Using the Lemma 2 from [2], we have: for $u > \frac{1}{e}$,

$$P[\frac{1}{n}N(\cdot) \geq eu\overline{P}_1] \leq \exp(-en\overline{P}_1 u \log u)$$

where $\overline{P}_1 = \frac{1}{v(\mathcal{Y}_m)}\sum_{i=1}^{v(\mathcal{Y}_m)} P(\epsilon_i \geq 0) \leq \exp[-2(1-2\gamma)^2(a-b)^2]$.

Step 3 Show that $\sup_\sigma \frac{1}{n}N(\cdot)$ is bounded by something.

Using Lemma 6 from [2], we have: for $\gamma \in (0,1)$, given n and γn are positive intergers,

$$\binom{n}{\gamma n} \leq \exp(nh(\gamma) + \kappa_\gamma(2n))$$

where $h(\gamma)$ is the binary entropy function, and $\kappa_\gamma(n) = \frac{1}{n}[\log\frac{n}{4\pi\gamma(1-\gamma)} + \frac{1}{3n}]$. Combine this with the conclusion from Step 2, we have:

$$P(\sup_\sigma \frac{1}{v(\mathcal{Y}_m)}N(\cdot) \geq eu\overline{P}_1) \leq \exp(v(\mathcal{Y}_m)[2h(\gamma) + 2\kappa_\gamma(2v(\mathcal{Y}_m))] - ev(\mathcal{Y}_m)\overline{P}_1\mu\log\mu)$$

Let $u = u_n$, we can construct a sequence u_n such that $u_n \log u_n = \frac{4h(\gamma)}{e\overline{P}_1}$. This finishes the proof and leads to the conclusion:

$$P[\sup_\sigma \frac{1}{v(\mathcal{Y}_m)}N(\cdot) \geq \frac{4h(\gamma)}{\log u_n}] \leq exp(-2v(\mathcal{Y}_m)[h(\gamma) - \kappa_\gamma(2v(\mathcal{Y}_m))])$$

Remark The boundary values $\frac{h(\gamma)}{\log\mu_n}$, as a function of γ, is shown in Figure 5. It is argued that as long as a is large enough, γ will goes to 1 [2].

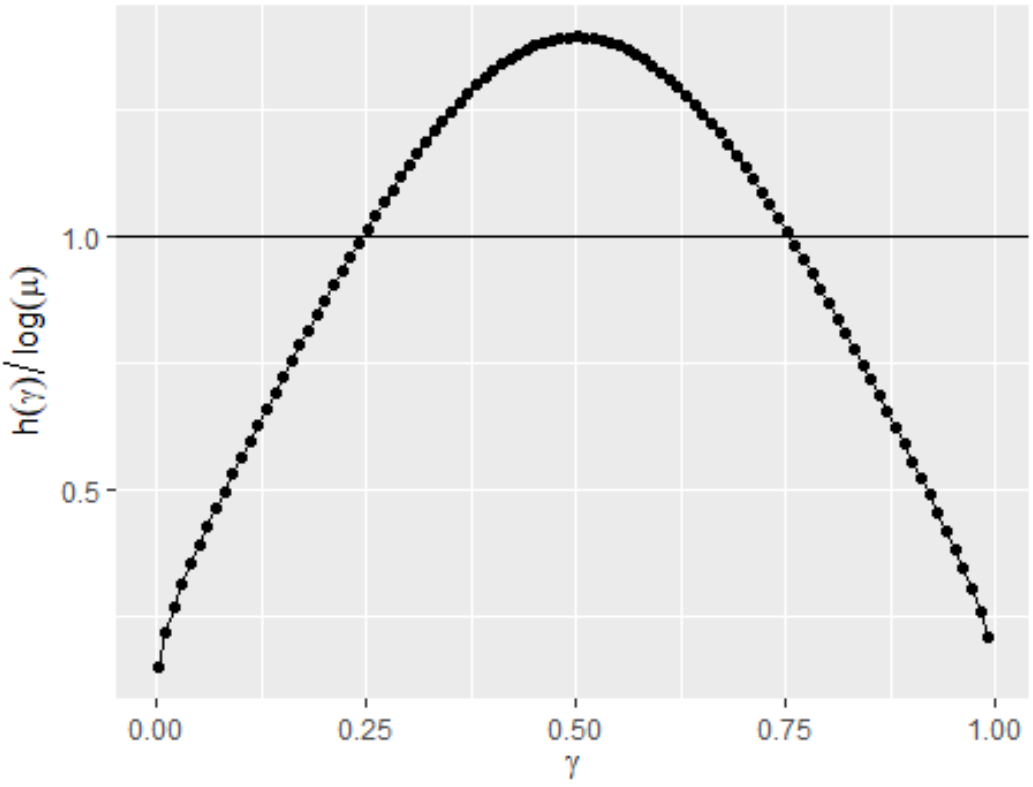

Figure 5: The visualization of $\frac{4h(\gamma)}{\log u_n}$. In this setting, $K = 2$, and the two clusters have the same power-law distribution parameters. We assume $a = 0.95$, $b = 0.05$. As γ goes to 0/1, $\frac{4h(\gamma)}{\log u_n}$ goes to 0.

6.2 Proof of Theorem 2

In this section, we are going to show given the sparsity of each sub-network, the sparsity retains in the overall network. We start by define $m(\mathcal{Y}_c, \mathcal{Y}_{c'})$ as the number of interactions between community c and c', $c, c' \in [K]$. Given the sparsity in all the sub-networks:

$$\limsup_{v(\mathcal{Y}_c)\to\infty} \frac{m(\mathcal{Y}_c)}{v(\mathcal{Y}_c)} = 0, \forall c \in [K]$$

we have:

$$\limsup_{v(\mathcal{Y}_m)\to\infty} \frac{m(\mathcal{Y}_m)}{v(\mathcal{Y}_m)}$$

$$= \limsup_{v(\mathcal{Y}_m)\to\infty} \frac{m(\mathcal{Y}_1) + m(\mathcal{Y}_2) +, ..., + m(\mathcal{Y}_K) + m(\mathcal{Y}_1, \mathcal{Y}_2) + ... + m(\mathcal{Y}_{K-1}, \mathcal{Y}_K)}{v(\mathcal{Y}_1) + v(\mathcal{Y}_2) + ... + v(\mathcal{Y}_K)}$$

$$= \limsup_{v(\mathcal{Y}_m)\to\infty} \frac{m(\mathcal{Y}_1) + m(\mathcal{Y}_2) + ... + m(\mathcal{Y}_K)}{v(\mathcal{Y}_1) + v(\mathcal{Y}_2) + ... + v(\mathcal{Y}_K)} + \limsup_{v(\mathcal{Y}_m)\to\infty} \frac{m(\mathcal{Y}_1, \mathcal{Y}_2) + ... + m(\mathcal{Y}_{K-1}, \mathcal{Y}_K)}{v(\mathcal{Y}_1) + v(\mathcal{Y}_2) + ... + v(\mathcal{Y}_K)}$$

$$\leq \limsup_{v(\mathcal{Y}_m)\to\infty} \frac{m(\mathcal{Y}_1)}{v(\mathcal{Y}_1)} + \limsup_{v(\mathcal{Y}_m)\to\infty} \frac{m(\mathcal{Y}_2)}{v(\mathcal{Y}_2)} + ... + \limsup_{v(\mathcal{Y}_m)\to\infty} \frac{m(\mathcal{Y}_1, \mathcal{Y}_2) + ... + m(\mathcal{Y}_{K-1}, \mathcal{Y}_K)}{v(\mathcal{Y}_1) + v(\mathcal{Y}_2) + ... + v(\mathcal{Y}_K)}$$

$$= 0 + \limsup_{v(\mathcal{Y}_m)\to\infty} \frac{m(\mathcal{Y}_1, \mathcal{Y}_2) + ... + m(\mathcal{Y}_{K-1}, \mathcal{Y}_K)}{v(\mathcal{Y}_1) + v(\mathcal{Y}_2) + ... + v(\mathcal{Y}_K)}$$

The first part of the equation goes to 0 given the sparsity assumption. Note that given the propensity matrix $\mathcal{B}$, the expectation of the interaction between clusters is $m(\mathcal{Y}_c) \times \frac{b}{a}$. The number of interactions between the two clusters is supposed to be the minimal of the two. Thus, by plugging in $a = \mu K b$, where μ is constant regarding the number of clusters, we have:

$$\limsup_{v(\mathcal{Y}_m)\to\infty} \frac{m(\mathcal{Y}_m)}{v(\mathcal{Y}_m)} = \frac{1}{\mu K} \limsup_{v(\mathcal{Y}_m)\to\infty} \frac{\min\{m(\mathcal{Y}_1), m(\mathcal{Y}_2)\} + \min\{m(\mathcal{Y}_1), m(\mathcal{Y}_3)\} + ... + \min\{m(\mathcal{Y}_{K-1}), m(\mathcal{Y}_K)\}}{v(\mathcal{Y}_1) + v(\mathcal{Y}_2) + ... + v(\mathcal{Y}_K)}$$

$$\leq \frac{1}{\mu K}(K-1)(\limsup_{v(\mathcal{Y}_m)\to\infty} \frac{m(\mathcal{Y}_1)}{v(\mathcal{Y}_1)} + \limsup_{v(\mathcal{Y}_m)\to\infty} \frac{m(\mathcal{Y}_2)}{v(\mathcal{Y}_2)} + ... + \limsup_{v(\mathcal{Y}_m)\to\infty} \frac{m(\mathcal{Y}_K)}{v(\mathcal{Y}_K)}) = 0$$

This finish the proof.

1,000 interactions	Paramters	$\{\alpha_c\} = \{0.1, 0.9\}$	$\{\alpha_c\} = \{0.2, 0.8\}$	$\{\alpha_c\} = \{0.3, 0.7\}$	$\{\alpha_c\} = \{0.4, 0.6\}$
$\{a, b\} = \{0.9, 0.1\}$	α_1	0.378 (0.110)	0.360 (0.106)	0.451 (0.113)	0.495 (0.077)
	α_2	0.908 (0.015)	0.809 (0.023)	0.694 (0.069)	0.611 (0.057)
	Diagonal	0.910 (0.021)	0.910 (0.020)	0.906 (0.019)	0.902 (0.019)
$\{a, b\} = \{0.7, 0.3\}$	α_1	0.409 (0.206)	0.511 (0.167)	0.479 (0.102)	0.520 (0.096)
	α_2	0.863 (0.124)	0.748 (0.112)	0.705 (0.051)	0.593 (0.066)
	Diagonal	0.716 (0.030)	0.728 (0.031)	0.714 (0.031)	0.705 (0.032)
$\{a, b\} = \{0.5, 0.5\}$	α_1	0.736 (0.214)	0.677 (0.128)	0.619 (0.091)	0.567 (0.082)
	α_2	0.757 (0.172)	0.718 (0.115)	0.629 (0.084)	0.573 (0.081)
	Diagonal	0.540 (0.052)	0.541 (0.057)	0.554 (0.061)	0.535 (0.057)
10,000 interactions	Paramters	$\{\alpha_c\} = \{0.1, 0.9\}$	$\{\alpha_c\} = \{0.2, 0.8\}$	$\{\alpha_c\} = \{0.3, 0.7\}$	$\{\alpha_c\} = \{0.4, 0.6\}$
$\{a, b\} = \{0.9, 0.1\}$	α_1	0.225 (0.072)	0.289 (0.062)	0.364 (0.04)	0.443 (0.038)
	α_2	0.901 (0.006)	0.803 (0.009)	0.707 (0.013)	0.614 (0.02)
	Diagonal	0.901 (0.006)	0.901 (0.006)	0.902 (0.005)	0.901 (0.006)
$\{a, b\} = \{0.7, 0.3\}$	α_1	0.258 (0.092)	0.408 (0.161)	0.411 (0.11)	0.448 (0.056)
	α_2	0.902 (0.005)	0.785 (0.066)	0.695 (0.054)	0.603 (0.032)
	Diagonal	0.704 (0.009)	0.674 (0.068)	0.691 (0.044)	0.694 (0.035)
$\{a, b\} = \{0.5, 0.5\}$	α_1	0.865 (0.163)	0.724 (0.162)	0.626 (0.095)	0.549 (0.059)
	α_2	0.703 (0.127)	0.657 (0.126)	0.637 (0.081)	0.555 (0.051)
	Diagonal	0.51 (0.015)	0.51 (0.015)	0.513 (0.017)	0.51 (0.017)

Table 3: Posterior means (SD) of power-law parameters $\{\alpha_c\}$ and within/between cluster propensity $\{a, b\}$ in different settings, with $\{\theta_1, \theta_2\} = \{10, 10\}$

6.3 Simulation results for varying values of $\{\theta_c\}$

In Section 3.2, we have shown the posteriors given $\theta_1 = \theta_2 = 5$. Though both $\{\alpha_c\}$ and $\{\theta_c\}$ are the power-law distribution parameters, the values of $\{\alpha_c\}$ have more contribution to the observed power-law properties. For the completeness, we show here the parameter estimates of the model parameters with varying values of θs. to be more specific, we have θs to be chosen from the following values: $\{\{10, 10\}, \{1, 1\}, \{10, 1\}, \{1, 10\}\}$. In all these settings, the conclusions based on the means of the posteriors are the similar to those when $\theta = \{5, 5\}$, with minor variations in the specific values.

1,000 interactions	Paramters	$\{\alpha_c\} = \{0.1, 0.9\}$	$\{\alpha_c\} = \{0.2, 0.8\}$	$\{\alpha_c\} = \{0.3, 0.7\}$	$\{\alpha_c\} = \{0.4, 0.6\}$
$\{a, b\} = \{0.9, 0.1\}$	α_1	0.218 (0.157)	0.224 (0.140)	0.304 (0.141)	0.354 (0.142)
	α_2	0.898 (0.015)	0.796 (0.031)	0.681 (0.052)	0.585 (0.064)
	Diagonal	0.908 (0.016)	0.885 (0.014)	0.892 (0.057)	0.897 (0.019)
$\{a, b\} = \{0.7, 0.3\}$	α_1	0.367 (0.281)	0.276 (0.221)	0.374 (0.203)	0.341 (0.157)
	α_2	0.870 (0.100)	0.782 (0.100)	0.689 (0.074)	0.580 (0.079)
	Diagonal	0.667 (0.078)	0.691 (0.06)	0.678 (0.063)	0.694 (0.046)
$\{a, b\} = \{0.5, 0.5\}$	α_1	0.386 (0.268)	0.442 (0.266)	0.414 (0.237)	0.348 (0.186)
	α_2	0.900 (0.050)	0.753 (0.153)	0.623 (0.128)	0.526 (0.132)
	Diagonal	0.519 (0.033)	0.521 (0.037)	0.519 (0.037)	0.517 (0.033)
10,000 interactions	Paramters	$\{\alpha_c\} = \{0.1, 0.9\}$	$\{\alpha_c\} = \{0.2, 0.8\}$	$\{\alpha_c\} = \{0.3, 0.7\}$	$\{\alpha_c\} = \{0.4, 0.6\}$
$\{a, b\} = \{0.9, 0.1\}$	α_1	0.157 (0.111)	0.218 (0.121)	0.274 (0.101)	0.395 (0.075)
	α_2	0.900 (0.006)	0.803 (0.012)	0.691 (0.025)	0.591 (0.032)
	Diagonal	0.900 (0.006)	0.899 (0.005)	0.900 (0.005)	0.900 (0.006)
$\{a, b\} = \{0.7, 0.3\}$	α_1	0.378 (0.351)	0.216 (0.120)	0.268 (0.132)	0.354 (0.117)
	α_2	0.873 (0.067)	0.802 (0.012)	0.687 (0.031)	0.586 (0.050)
	Diagonal	0.653 (0.078)	0.693 (0.038)	0.660 (0.078)	0.680 (0.052)
$\{a, b\} = \{0.5, 0.5\}$	α_1	0.732 (0.262)	0.597 (0.259)	0.521 (0.199)	0.351 (0.191)
	α_2	0.853 (0.121)	0.721 (0.138)	0.672 (0.081)	0.567 (0.073)
	Diagonal	0.506 (0.011)	0.507 (0.012)	0.505 (0.011)	0.505 (0.010)

Table 4: Posterior means (SD) of power-law parameters $\{\alpha_c\}$ and within/between cluster propensity $\{a, b\}$ in different settings, with $\{\theta_1, \theta_2\} = \{1, 1\}$

1,000 interactions	Paramters	$\{\alpha_c\} = \{0.1, 0.9\}$	$\{\alpha_c\} = \{0.2, 0.8\}$	$\{\alpha_c\} = \{0.3, 0.7\}$	$\{\alpha_c\} = \{0.4, 0.6\}$
$\{a, b\} = \{0.9, 0.1\}$	α_1	0.212 (0.151)	0.297 (0.196)	0.354 (0.181)	0.384 (0.14)
	α_2	0.903 (0.016)	0.808 (0.038)	0.718 (0.054)	0.626 (0.049)
	Diagonal	0.900 (0.019)	0.887 (0.079)	0.885 (0.08)	0.899 (0.018)
$\{a, b\} = \{0.7, 0.3\}$	α_1	0.381 (0.312)	0.367 (0.232)	0.382 (0.201)	0.358 (0.152)
	α_2	0.895 (0.054)	0.781 (0.119)	0.704 (0.081)	0.633 (0.048)
	Diagonal	0.668 (0.079)	0.672 (0.074)	0.679 (0.065)	0.689 (0.05)
$\{a, b\} = \{0.5, 0.5\}$	α_1	0.548 (0.308)	0.502 (0.25)	0.568 (0.202)	0.5 (0.169)
	α_2	0.871 (0.122)	0.806 (0.076)	0.671 (0.119)	0.589 (0.101)
	Diagonal	0.513 (0.034)	0.526 (0.04)	0.518 (0.039)	0.525 (0.039)
10,000 interactions	Paramters	$\{\alpha_c\} = \{0.1, 0.9\}$	$\{\alpha_c\} = \{0.2, 0.8\}$	$\{\alpha_c\} = \{0.3, 0.7\}$	$\{\alpha_c\} = \{0.4, 0.6\}$
$\{a, b\} = \{0.9, 0.1\}$	α_1	0.143 (0.101)	0.186 (0.104)	0.31 (0.103)	0.396 (0.075)
	α_2	0.901 (0.006)	0.803 (0.011)	0.709 (0.013)	0.61 (0.018)
	Diagonal	0.899 (0.006)	0.900 (0.006)	0.900 (0.006)	0.899 (0.007)
$\{a, b\} = \{0.7, 0.3\}$	α_1	0.354 (0.319)	0.391 (0.262)	0.433 (0.195)	0.42 (0.113)
	α_2	0.900 (0.028)	0.794 (0.041)	0.694 (0.047)	0.609 (0.024)
	Diagonal	0.656 (0.081)	0.649 (0.081)	0.647 (0.075)	0.666 (0.069)
$\{a, b\} = \{0.5, 0.5\}$	α_1	0.751 (0.271)	0.629 (0.229)	0.596 (0.164)	0.531 (0.122)
	α_2	0.844 (0.109)	0.787 (0.06)	0.683 (0.08)	0.59 (0.063)
	Diagonal	0.506 (0.011)	0.508 (0.012)	0.506 (0.012)	0.508 (0.013)

Table 5: Posterior means (SD) of power-law parameters $\{\alpha_c\}$ and within/between cluster propensity $\{a, b\}$ in different settings, with $\{\theta_1, \theta_2\} = \{1, 10\}$

1,000 interactions	Paramters	$\{\alpha_c\} = \{0.1, 0.9\}$	$\{\alpha_c\} = \{0.2, 0.8\}$	$\{\alpha_c\} = \{0.3, 0.7\}$	$\{\alpha_c\} = \{0.4, 0.6\}$
$\{a, b\} = \{0.9, 0.1\}$	α_1	0.323 (0.099)	0.368 (0.091)	0.402 (0.064)	0.485 (0.078)
	α_2	0.893 (0.028)	0.789 (0.036)	0.691 (0.052)	0.582 (0.094)
	Diagonal	0.914 (0.02)	0.904 (0.02)	0.906 (0.019)	0.896 (0.022)
$\{a, b\} = \{0.7, 0.3\}$	α_1	0.369 (0.129)	0.459 (0.154)	0.46 (0.097)	0.477 (0.083)
	α_2	0.896 (0.024)	0.75 (0.099)	0.636 (0.101)	0.553 (0.097)
	Diagonal	0.702 (0.054)	0.714 (0.03)	0.711 (0.03)	0.701 (0.043)
$\{a, b\} = \{0.5, 0.5\}$	α_1	0.49 (0.222)	0.556 (0.19)	0.508 (0.157)	0.466 (0.142)
	α_2	0.859 (0.099)	0.665 (0.145)	0.576 (0.095)	0.546 (0.084)
	Diagonal	0.528 (0.044)	0.524 (0.048)	0.53 (0.047)	0.52 (0.045)
10,000 interactions	Paramters	$\{\alpha_c\} = \{0.1, 0.9\}$	$\{\alpha_c\} = \{0.2, 0.8\}$	$\{\alpha_c\} = \{0.3, 0.7\}$	$\{\alpha_c\} = \{0.4, 0.6\}$
$\{a, b\} = \{0.9, 0.1\}$	α_1	0.203 (0.067)	0.297 (0.056)	0.345 (0.042)	0.44 (0.03)
	α_2	0.900 (0.006)	0.798 (0.012)	0.697 (0.022)	0.586 (0.034)
	Diagonal	0.902 (0.006)	0.900 (0.007)	0.900 (0.007)	0.878 (0.085)
$\{a, b\} = \{0.7, 0.3\}$	α_1	0.286 (0.177)	0.302 (0.082)	0.343 (0.093)	0.442 (0.064)
	α_2	0.882 (0.082)	0.795 (0.018)	0.682 (0.041)	0.563 (0.056)
	Diagonal	0.692 (0.044)	0.686 (0.051)	0.668 (0.065)	0.639 (0.087)
$\{a, b\} = \{0.5, 0.5\}$	α_1	0.72 (0.265)	0.403 (0.181)	0.507 (0.156)	0.466 (0.094)
	α_2	0.726 (0.172)	0.776 (0.059)	0.603 (0.092)	0.531 (0.054)
	Diagonal	0.507 (0.012)	0.508 (0.012)	0.507 (0.013)	0.509 (0.013)

Table 6: Posterior means (SD) of power-law parameters $\{\alpha_c\}$ and within/between cluster propensity $\{a, b\}$ in different settings, with $\{\theta_1, \theta_2\} = \{10, 1\}$

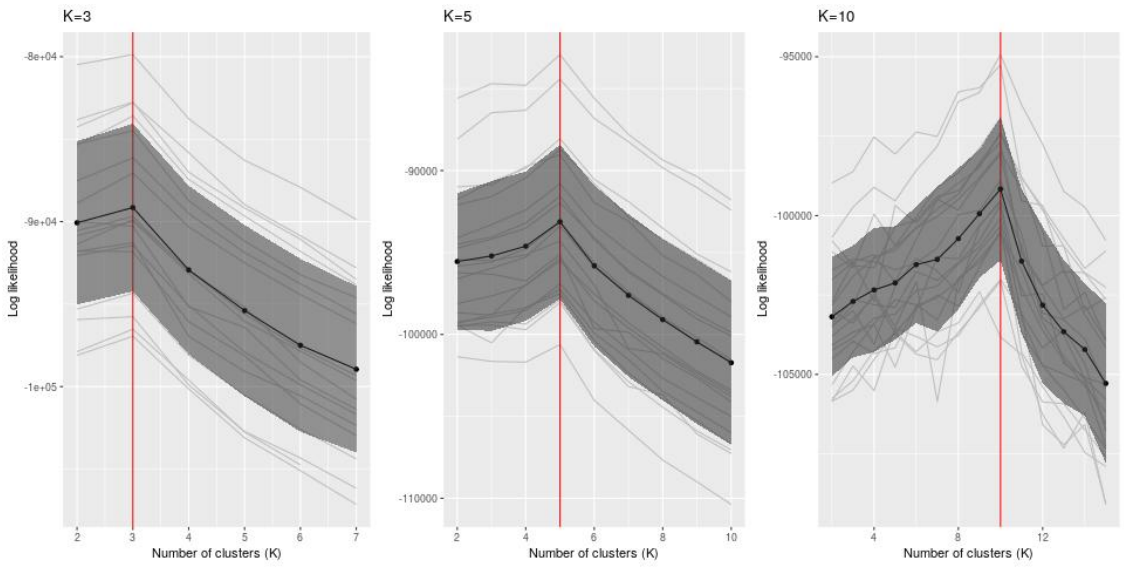

Figure 6: The trace plot of the log likelihood over different selection of K. The grey lines represent results from different sets. The black line is the average over different sets. The red vertical line is the underlying truth in the generative model.

6.4 Marginal likelihood over varying K

We propose a model selection method in Section 3.4. Here, we provide the simulation results to support our arguments. To begin with, we simulate 10,000 interactions in total and set the number of clusters K to be 3, 5, and 10 correspondingly. The values of α are randomly chosen from $Uniform(0.4, 0.8)$, and θ is set to be 5. The intra-cluster connectivity is set to be $a = 0.9$, while the inter-cluster connectivity is set to be $b = 0.2/(K-1)$. We calculate the marginal log likelihood (Eq 3) of the model corresponding to different Ks in the running model. The procedure is repeated for 20 times. The results are shown in Figure 6. Though there are variations in the values of likelihood in different settings, the marginal likelihood given by the Eq 3 always hit the largest value when K is equal to the underlying truth.

6.5 Case study with model fitting in other network

In Section 4, we showed two examples using Alcohol and Substance Abuse network and Behavoiral Symptoms network. Note that not all the networks will give proper results due to the complexity of the underlying community structure. Here, we showed the results from fitting several more

networks in Figure 7, including Body Imagining Eating Disorder Suspected network and Nssi Urge Suspected network. Our main conclusions remain the same as stated in the main context.

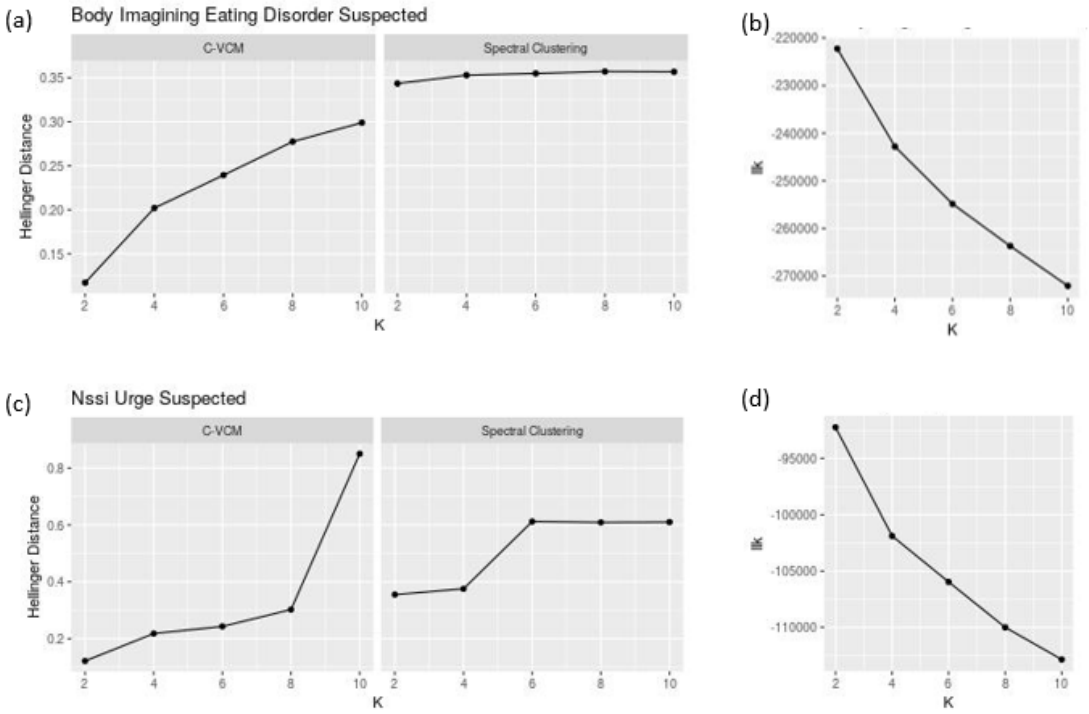

Figure 7: The Hellinger distances of the cluster assignment between the first half and the second half of the 2019 data in (a) Body Imagining Eating Disorder Suspected network and (c) Nssi Urge Suspected network. The marginal likelihood over different K values in (b) Body Imagining Eating Disorder Suspected network and (d) Nssi Urge Suspected network.